RESEARCH ARTICLE

H_∞ Loop-Shaping Continuous-Time Controller Design for Nonlinear HDD Systems: A Reduced-Order Approach Using Hankel-Norm Approximation

IBRAHIM SHAIKH, RADEK MATUŠŮ, (Member, IEEE), EL WARDI ZERDAZI, AND ABEBE ALEMU WENDIMU

Department of Automation and Control Engineering, Tomas Bata University in Zlín, 760 01 Zlín, Czech Republic

Corresponding author: Ibrahim Shaikh (shaikh@utb.cz)

ABSTRACT This study presents the development and examination of a streamlined H_∞ loop-shaping continuous-time controller tailored for nonlinear Hard Disk Drive (HDD) systems. Using the Hankel-norm approximation technique, the complexity of the controller is systematically reduced, emphasizing preserving the system's efficacy while enhancing computational efficiency. The dynamics of the HDD system and the performance of the proposed controller are investigated through MATLAB simulations. The effectiveness of the controller is quantitatively measured by employing the ITAE (Integral of Time multiplied by Absolute Error) criterion. The results indicate that a controller of the 10th-order provides a desirable compromise between maintaining robust control and minimizing disturbances and noise without significant loss in performance. This method illustrates the capacity for implementing more straightforward controllers in complex HDD systems, paving the way for their application in precision-critical industrial settings.

INDEX TERMS Nonlinear HDD systems, reduced-order continuous-time controller, H_∞ loop-shaping, Hankel-norm approximation, MATLAB simulation.

I. INTRODUCTION

The HDD systems play a crucial role in data storage and retrieval processes. Despite the advent of SSD (Solid State Drive) technology, HDD remains pivotal in scenarios necessitating vast storage spaces and economic feasibility, attributed to their mechanical design. As the demand for swifter and more reliable HDDs escalates, the control mechanisms that oversee their functionality have emerged as a focal point of analysis.

The development of HDD control systems has seen significant advancements, focusing on improving performance and reducing complexity. Several studies have explored various control methods to enhance the precision and

The associate editor coordinating the review of this manuscript and approving it for publication was Jinquan Xu.

efficiency of HDD systems. This paper presents a streamlined H∞ loop-shaping continuous-time controller for nonlinear HDD systems, leveraging the Hankel-norm approximation technique to reduce controller complexity while maintaining performance.

Recent literature highlights several advancements in HDD control systems. For instance, a loop-shaping technique for quadruple-stage actuator systems in HDDs, utilizing Robust Bode plots, enhanced positioning accuracy and robustness against large disturbances [1]. Additionally, a feedforward control method using a sampled-data polynomial based on a causal first-order hold reduced seek time in HDDs, outperforming the conventional zero-order hold [2].

Furthermore, a convex optimization-based robust mixed H_2-H_∞ control synthesis method for dual-stage hard disk drives effectively minimized the piezoelectric micro-actuator

stroke variance while ensuring robustness, although further research is needed to validate performance across a broader range of operational conditions [3]. Clustering techniques for stable linear dynamical systems applied to HDDs, using k-medoids and Gaussian Mixture Models (GMM), enhanced controller performance by addressing variations within clusters [4].

Moreover, a fixed-structure H∞ controller optimization technique for tuning PID controllers in HDD head positioning systems enhanced positioning accuracy without requiring extensive manual loop-shaping expertise [5]. A data-driven loop shaping method tailored to dual-stage actuator magnetic head positioning control systems in HDDs employed support vector machines (SVMs) for filter design, effectively enhancing disturbance suppression and positioning accuracy [6].

A cost-effective optical beam shutter using a hard disk drive voice-coil actuator achieved opening and closing delay response time, providing comparable performance to commercial alternatives at a fraction of the cost, though further optimization is needed for real-time applications [7]. An optimized resonant filter design for disturbance rejection in dual-stage actuator hard disk drives significantly improved track-following performance using frequency response data and iterative convex optimization, although further validation across diverse HDD models is necessary [8].

Additionally, an adaptive control system for HDD servo mechanisms incorporating a PID controller tuned using the normalized MIT rule improved head positioning accuracy and response speed but requires further testing under real-world conditions [9]. An adaptive tuning and control system for hard disk drives utilizing a model-based adaptive loop integrated with an LTI stabilizing controller to minimize position control error presented two methods: control tuning and real-time fully adaptive control (RTFAC), both showing significant improvements in disturbance rejection and convergence speed [10].

A servo controller design for triple-stage actuator HDDs aimed at mitigating high-frequency vibrations caused by cooling fans in data servers leveraged increased feedback gain for VCM and milliactuators, achieving up to 58% improvement in positioning accuracy [11]. A Nonlinear Model Predictive Control (NMPC) approach for the voice-coil motor in HDDs showed superior performance in track following compared to traditional PID controllers, particularly under disturbances and parameter uncertainties [12]. Similarly, an evolutionary-based optimization technique for tuning the PID controller in HDD head positioning systems, utilizing Genetic Algorithm (GA) and Particle Swarm Optimization (PSO), demonstrated significant improvements in transient performance and error reduction [13]. A self-tuning fuzzy PID (STFL-PID) controller for HDD servo control with time delay demonstrated superior performance compared to conventional PID and fuzzy logic PD controllers, significantly improving control accuracy [14].

A high-bandwidth control system for a dual-stage actuation HDD using a novel microthermal actuator demonstrated a significant bandwidth increase seeking time for steps [15]. Furthermore, a coupling controller design for the multi-input single-output (MISO) head positioning control system in HDDs enhanced positioning accuracy by 31% compared to conventional decoupling methods, offering greater flexibility and performance gains [16].

Various controller reduction methods, such as balanced truncation, balanced residualization, and Hankel norm approximation, have been employed to simplify controller design while preserving essential dynamics. Balanced truncation and balanced residualization techniques are generally easier to implement and are effective for a wide range of applications, particularly in mid-range frequency domains. However, they might fall short in systems requiring high-frequency precision or guaranteed performance metrics [17]. In contrast, Hankel norm approximation, though more complex, excels in preserving system stability and performance, making it ideal for high-precision applications like advanced HDD control systems. The choice of reduction method depends on the specific requirements of the system, such as the frequency range of interest, computational resources, and the criticality of maintaining performance and stability [18].

Our research addresses building upon the gaps identified in previous works [19]. Therefore, this paper aims to fill the gaps by presenting a comparative solution.

The main contributions of this paper are:
1) Development of a 10th-order H∞ loop-shaping continuous-time controller for nonlinear HDD systems using Hankel-norm approximation.
2) Comprehensive evaluation of the controller's performance using various performance criteria, including ITAE (Integral of Time multiplied by Absolute Error), ISE (Integral of Square Error), and IAE (Integral of Absolute Value of Error).
3) Detailed comparative analysis of controllers with different orders to identify the optimal controller order for various application scenarios.
4) Validation of the controller's robustness and adaptability through multi-scenario simulations using MATLAB and Simulink.

The findings indicate that a 10th-order controller provides a desirable compromise between maintaining robust control and minimizing disturbances and noise without significant performance loss. This approach highlights the potential for implementing more straightforward controllers in complex HDD systems, paving the way for their application in precision-critical industrial settings.

The paper is structured as follows: Section II discusses system modeling, while Section III delves into the controller design, emphasizing the Hankel-norm approximation method. Section IV presents the simulation results and a discussion on the performance of the 10th-order controller.

Finally, Section V concludes the paper, summarizing our findings and suggesting future research directions.

II. SYSTEM MODELING

Modeling the HDD system within the context of control systems typically involves constructing a mathematical depiction of the HDD's servo system mechanism. This mechanism is responsible for accurately and swiftly positioning the read-write head at the exact spot on the disk platter. The model encompasses the dynamics of both mechanical and electrical components of the HDD and plays a vital role in the development of control systems [21]. Understanding and accurately modeling these dynamics are essential for designing effective control strategies that can enhance the performance and reliability of HDD systems by the equation

$$J \frac{d^2\theta}{dt^2} = t_m + t_d, \qquad (1)$$

where J is the moment of inertia of the arm, and θ represents the rotation angle of the arm. The torque generated by the VCM (Voice Coil Motor), denoted as t_m, plays a crucial role in the system dynamics. Additionally, the system is subjected to a disturbance torque t_d, which has a magnitude of 0.0005 Nm. This disturbance torque is an external factor influencing the system behavior, and the VCM torque is the actuating force counteracting this disturbance. The behavior of the rotary arm, a key element in the HDD's operation. Equation (2) provides a relationship between t_m and i_c (current in the VCM coil)

$$t_m = k_t i_c, \qquad (2)$$

where k_t denotes the motor torque constant and the voice coil is characterized by its inherent electrical properties, specifically a resistance R_{coil} and an inductance L_{coil}.
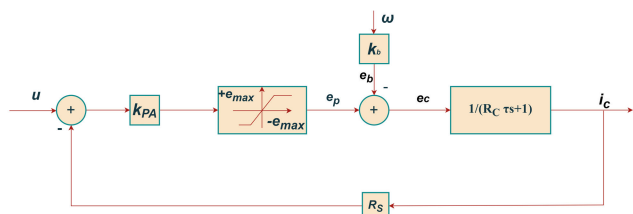

FIGURE 1. Block diagram representation of the power amplifier linked to the voice coil [21].

A current sensing resistor, denoted as R_s, is integrated in series with the voice coil circuit to enable feedback from the power amplifier's output. Consequently, the electrical admittance of the voice coil can be described through a corresponding transfer function. The torque generated by the VCM, which is a critical component in the system dynamics, is derived from this configuration.

$$G_{vca}(s) = \frac{i_c(s)}{e_c(s)} = \frac{1}{R_c} \frac{1}{\tau s + 1}, \qquad (3)$$

where e_c represents the voltage applied to the voice coil. The time constant τ is defined as $\frac{L_{\text{coil}}}{R_c}$, where R_c is the total resistance in the circuit, calculated as $R_{\text{coil}} + R_s$.

The arc length, associated with the rotation angle of the arm θ, is defined by $R\theta$. For small angles θ, the number of tracks covered by the arc can be expressed as $R \times \theta_{pm}$, leading to a derived output signal.

$$y = R \cdot \theta_{pm} \cdot k_y \cdot \theta. \qquad (4)$$

Neglecting the voice coil's dynamics allows the servo actuator to be modeled as a rigid entity, represented by a transfer function analogous to a double integrator. However, this oversimplification of system dynamics may not provide reliable results for design purposes. The analysis progresses by incorporating the high-frequency resonance modes of the head disk assembly, which are encapsulated within the transfer function $H_d(s)$. In the given context, $H_d(s)$ encompasses four distinct resonance modes, and is formulated as

$$H_d(s) = \sum_{j=q=1}^{4} \frac{b_{2j}\omega_j s + b_{2j-1}\omega_q^2}{s^2 + 2\zeta_j\omega_j s + \omega_q^2}. \qquad (5)$$
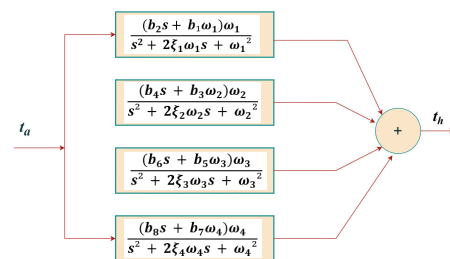

FIGURE 2. Transfer functions of resonant modes [21].

Referencing Fig. 2, ω_j, ζ_j, and b_{2j}, b_{2j-1} sequentially represent the resonance frequency, damping ratio, and coupling coefficients for the jth mode, where j ranges from 1 to 4.

TABLE 1. Parameters of the rigid body model [21].

Parameter	Description	Value	Units
J	arm moment of inertia	6.3857×10^{-6}	kg m^2
R	arm length	5.08×10^{-2}	m
k_{PA}	amplifier gain	10.0	V/V
k_t	VCM torque constant	9.183×10^{-2}	Nm/A
k_b	back e.m.f. constant	9.183×10^{-2}	Nm/A
tpm	tracks per meter	10^6	tracks
k_y	position measurement gain	1.2	V/track
R_{coil}	coil resistance	8.00	Ω
R_s	Sense resistance	0.2	Ω
L_{coil}	coil inductance	0.001	H
e_{max}	saturated power amplifier voltage	12.0	V
rpm	disk rotation rate	7200	rev/min
t_w	track width	1	μm

Implementing robust control strategies necessitates a comprehensive plant model encompassing various parameters. An analysis of Table 1 and 2 reveals that the total number of parameters surpasses 25, presenting a challenge in studying and developing HDD servo systems. This research aims to

TABLE 2. Parameters of resonance [21].

Parameter	Description	Value	Units
ω_1	pivot bearing resonance	$2\pi50$	rad/s
ω_2	first torsional resonance	$2\pi2200$	rad/s
ω_3	second torsional resonance	$2\pi6400$	rad/s
ω_4	first sway resonance	$2\pi8800$	rad/s
b_1	first resonance coupling	0.006	1/s
b_2	first resonance coupling	0.000	-
b_3	second resonance coupling	0.013	-
b_4	second resonance coupling	-0.0018	1/s
b_5	third resonance coupling	0.723	-
b_6	third resonance coupling	-0.0015	1/s
b_7	fourth resonance coupling	0.235	-
b_8	fourth resonance coupling	-0.0263	1/s
ξ_1	first resonance damping	0.05	-
ξ_2	second resonance damping	0.024	-
ξ_3	third resonance damping	0.129	-
ξ_4	fourth resonance damping	0.173	-

concentrate on the parameters that profoundly impact the efficacy of the closed-loop system.

During the dynamic simulation of the HDD system, several parameters and conditions are crucial for evaluating the controller's performance. These include:

Torque Constants (k_t): The torque generated by the Voice Coil Motor (VCM) directly affects the actuator's response.

Inertia (J): The moment of inertia of the actuator arm influences the dynamics of the system.

Damping Ratios (ζ_j): The damping characteristics of the system's mechanical components are critical for ensuring stability and minimizing oscillations.

Resonance Frequencies (ω_j): High-frequency resonance modes must be accurately modeled to predict and mitigate potential vibrations.

Disturbance Torque (t_d): External disturbances, such as mechanical shocks, must be considered to evaluate the robustness of the controller.

Noise Levels: Sensor noise impacts the accuracy of position feedback and overall system performance.

These parameters were meticulously adjusted to reflect realistic operating conditions and comprehensively evaluate the controller's performance.
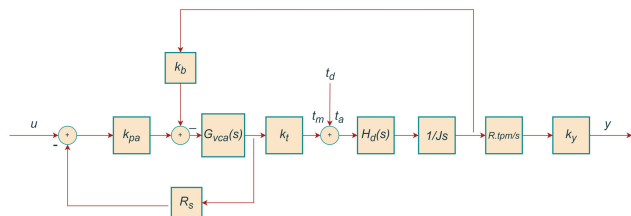

FIGURE 3. Block diagram representation of the system [21].

Fig. 3 presents the block diagram of the plant under consideration. The initial step involves developing the model for the resonance modes, where a similar transfer function structure characterizes each of the four modes. There are multiple methodologies for deriving this model, one of which

includes the approach depicted in Fig. 3.

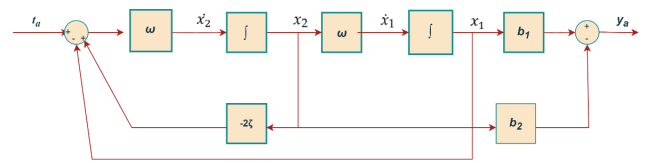$$\dot{x}_1 = \omega x_2. \tag{6}$$

FIGURE 4. Block diagram representation of a resonant model [21].

The function can construct a transfer function for each resonance mode. In this case, the parameter ω appears fivefold, leading to model parameters and thereby intricating both the analytical review and the synthesis of the system. To mitigate this complexity, the current study adopts a state-space formulation where ω is featured merely twice. This approach facilitates a more streamlined depiction of a resonance mode within the state-space framework. Fig. 4 illustrates the integrated representation of all four resonance modes.

FIGURE 5. Block diagram representation of the HDD regarded as a control system [21].

After establishing the transfer functions for the resonance modes, the uncertain plant model is constructed using the `iconnect` function, which leverages the block diagram depicted in Fig. 3. The HDD model is defined by a dual-input, single-output setup, as illustrated in Fig. 5.

Hence, the representation

$$G = [G_d \quad G_u] \tag{7}$$

and

$$y = G_d t_d + G_u u. \tag{8}$$

In this context, G_d and G_u denote the scalar transfer functions of the plant relative to the disturbance and control inputs respectively. The Bode plot for the HDD is illustrated in Fig. 6.

III. CONTROLLER DESIGN

Addressing the challenges inherent in precisely controlling nonlinear HDD systems, our approach concentrated on developing a reduced-order H_∞ loop-shaping controller. The following section elaborates on the strategies employed during the design process of the controller.
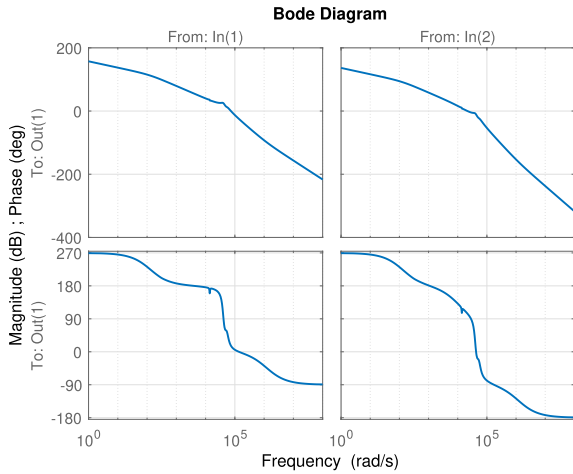
FIGURE 6. Bode plot representation of the HDD under disturbance and control action.

A. STRUCTURE OF THE CONTROL SYSTEM

Fig. 7 showcases the system's internal structure with four inputs and three outputs, encapsulated within the variable `sys_ic`. The variables `ref`, `dist`, and `noise` correspond to the reference signal, perturbation, and interference, respectively, while `control` denotes the actuation signal and emphasis on the variables `ref`, `dist`, `noise`, `y`, and `y_c`. The construction of the open-loop connection is facilitated by an M-file in Matlab, with the diagram in Fig. 7 elucidating the specific input-output configuration associated with `sys_ic`.
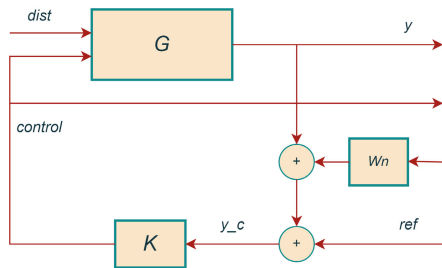

FIGURE 7. Schematic representation of the closed-loop system [21].

The function for shaping noise W_n is established based regarding the spectral density of the position noise signal. In the specified instance, it is assumed as the high-pass filter [21]:

$$W_n = \frac{6 \times 0.0001\,(0.1s + 1)}{0.001s + 1}. \tag{9}$$

Significant spectral components above 500 Hz characterize the system's output. Within this filtering technique, the position noise signal is relatively low at 0.6 mV in the lower frequency ranges but escalates to 60 mV at higher frequencies. This increase corresponds to a positional error amounting to 5% of the track width.

To align with the transfer function G_{nom} the transfer function representing the nominal open-loop system,

the variable `hin_ic` is obtained through the command: `hin_ic = sys_ic.Nom`. In the design process, a prefilter W_1 and a postfilter W_2 are utilized to appropriately modulate the frequency response of the enhanced open-loop transfer function $W_2 G W_1$. Consequently, the prefilter is chosen to have a transfer function [21]:

$$W_1 = \frac{0.2s + 4}{s}. \tag{10}$$

To guarantee a minimal steady-state error induced by perturbations under 10% of the track width, a gain factor of 4 is chosen. While a higher gain can further diminish steady-state errors, it may adversely affect the system's transient response. The postfilter is designated as $W_2 = 1$. Fig. 8 compares the amplitude responses of both the original and the adjusted systems. The development of the H_∞ loop-shaping controller is facilitated by the M-file `lshp_hdd`, which employs the `ncfsyn` function. The resultant controller, with an order of 13, aligns with the intended maximum order for the controller.

B. METHOD FOR REDUCING CONTROLLER ORDER (HANKEL-NORM APPROXIMATION)

Reducing the controller order through Hankel-norm approximation combines systems theory and model reduction methodologies. This technique for simplifying the H_∞ loop-shaping controller is based on several key factors:

- **Preservation of Essential Dynamics**: Retains the critical control characteristics necessary for robust performance.
- **Computational Efficiency**: Reduces the controller order, enhancing computational efficiency without significantly compromising performance.
- **Balance Between Performance and Complexity**: Achieves a simplified, manageable model by retaining dominant system dynamics and truncating less significant ones.
- **Robustness and Stability**: Ensures that the reduced-order controller maintains performance across varying operating conditions.

The Hankel-norm approximation impacts controller performance through the following steps:

- **System Representation**: Represents the original high-order system in a balanced state-space form to ensure equal and diagonal Gramians.
- **Singular Value Decomposition (SVD)**: Identifies and separates significant dynamics from less critical ones, allowing for the truncation of states.
- **Truncation of States**: Reduces controller complexity and computational load by truncating states with smaller singular values.
- **Reconstruction of Reduced-Order Model**: Preserves the essential dynamics of the original system while reconstructing the reduced-order model.

- **Controller Synthesis**: Uses the reduced-order model to synthesize the H_∞ loop-shaping controller, meeting performance objectives like disturbance rejection and noise attenuation.
- **Performance Evaluation**: Evaluates the reduced-order controller's performance through simulations using metrics such as ITAE, transient response, and control effort.

The Hankel-norm approximation technique was chosen for its ability to preserve essential system dynamics, enhance computational efficiency, and maintain robust performance, making it ideal for simplifying the H_∞ loop-shaping controller for nonlinear HDD systems. Mathematically describe below.

C. APPROXIMATION 1

Let $G(S)$ represent a stable and balanced system (HDD), characterized by a state-space representation $[A, B, C, D]$ that is minimal and balanced. Assume the Gramians P and Q to be equal and defined as $P = Q = \text{diag}(\Sigma_1, \sigma I_l)$, with σ representing the smallest Hankel singular value of multiplicity l, and each entry of Σ_1 being greater than σ. By partitioning $[A, B, C]$ appropriately, an $(n - l)$th-order system $G_h(s)$ can be constructed as detailed in [21]. The process involves

$$\hat{A} = \Gamma^{-1}(\sigma^2 A_{11}^T + \Sigma_1 A_{11}\Sigma_1 - \sigma C_1^T U B_1^T), \quad (11)$$

$$\hat{B} = \Gamma^{-1}(\Sigma_1 B_1 + \sigma C_1^T U), \quad (12)$$

$$\tilde{C} = C_1 E_1 + \alpha U B^T, \quad (13)$$

$$\tilde{D} = D - \alpha U. \quad (14)$$

where U represents an orthonormal matrix that fulfills

$$B_2 = -C_2^T U, \quad (15)$$

and

$$\Gamma = E_1^2 - \sigma I. \quad (16)$$

The reduced-order system $G_h(s)$ is defined as

$$G_h(s) = \tilde{C}(sI - A)^{-1}\tilde{B} + \tilde{D}. \quad (17)$$

It is the $(n - l)$-th order $G_h(s)$ is stable and is an optimal approximation of $G(s)$ satisfying

$$\|G(s) - G_h(s)\|_H = \sigma. \quad (18)$$

And, it is also true that $G(s) - G_h(s)$ is all-pass with the inf-norm

$$\|G(s) - G_h(s)\|_\infty = \sigma. \quad (19)$$

D. APPROXIMATION 2

It can be demonstrated that the Hankel singular values of $G_h(s)$ outlined in (16) are respectively identical to those initial $(n - l)$ Hankel singular values of $G(s)$. Therefore, the reduction above equation can be successively utilized to obtain additional reduced-order systems with established error margins.

Let the Hankel singular values of $G(s)$ be $\sigma_1 > \sigma_2 > \cdots > \sigma_r$, with multiplicities

E. APPROXIMATION 3

Let the Hankel singular values of $G(s)$ be $\sigma_1 \geq \sigma_2 \geq \cdots \geq \sigma_k > \sigma_{k+1} = \cdots = \sigma_{k+l} > \sigma_{k+l+1} \geq \cdots \geq \sigma_n$. Apply appropriate state similarity transformations to make the Gramians of $G(s)$ be arranged as

$$\Sigma = \text{diag}(\sigma_1, \sigma_2, \ldots, \sigma_k, \sigma_{k+1}, \ldots, \sigma_n, \sigma_{k+1}, \ldots, \sigma_{k+l})$$

Define the last l Hankel singular values to be σ. Following the equations from (11) to (16), define an $(n-l)$-th order $G(s)$. This $G(s)$ is not stable but has exactly k stable poles. The k-th order stable part $G_{h}, k(s)$ of $G(s)$, obtained by using modal decompositions say, is an k-th order Hankel optimal approximation of $G(s)$ and satisfies

$$\|G(s) - G_{h,k}(s)\|_H = \sigma.$$

Nonsquare plants can be augmented with zero column rows and applied using the above procedures.

F. INTEGRAL OF TIME MULTIPLIED BY ABSOLUTE ERROR (ITAE)

The ITAE criterion focuses on minimizing both the magnitude and duration of errors, guiding the selection of controller order. The 10th-order controller, with its minimal ITAE value, demonstrates significant potential for enhancing data integrity and operational performance in HDD environments. The ITAE criterion is mathematically defined as follows [20]:

$$ITAE = \int_0^\infty t \cdot |e(t)| \, dt, \quad (20)$$

where t represents the time elapsed since initiating a step input, and $e(t)$ denotes the absolute value of the error signal at time t, typically indicating the deviation between the desired and actual system outputs.

Advantages of ITAE in Controller Performance Evaluation

- **Emphasis on Long-Term Errors**: ITAE places greater weight on persistent errors, making it effective in reducing steady-state errors and enhancing system stability.
- **Balanced Performance**: By minimizing the time-multiplied absolute error, ITAE ensures a balanced trade-off between quick response and minimal overshoot.
- **Practical Relevance**: ITAE is particularly useful in applications requiring long-term accuracy, such as HDD systems where data integrity over extended operation is crucial.

Comparison with Other Performance Criteria

- **ISE**: ISE minimizes the sum of squared errors, making it sensitive to large errors but potentially more sensitive to noise. It is defined as:

$$ISE = \int_0^\infty e^2(t) \, dt. \quad (21)$$

- **IAE** : IAE minimizes the sum of absolute errors, providing a straightforward measure of overall error magnitude but may not adequately penalize persistent errors. It is defined as:

$$IAE = \int_0^\infty |e(t)|\, dt. \qquad (22)$$

The controller's performance was robust across ITAE, ISE, and IAE criteria, confirming its suitability for precision-critical applications. ITAE provided the most balanced performance, ensuring minimal steady-state error while maintaining robust transient response characteristics.

IV. SIMULATION RESULTS AND DISCUSSION

The design of reduced-order H_∞ loop-shaping continuous-time controllers and Hankel-norm approximation has undergone thorough examination for nonlinear HDD systems. The principal aim revolves around optimizing the trade-off between computational efficiency and the system's overall performance, alongside maintaining effective, robust control amidst various disturbances and noise.
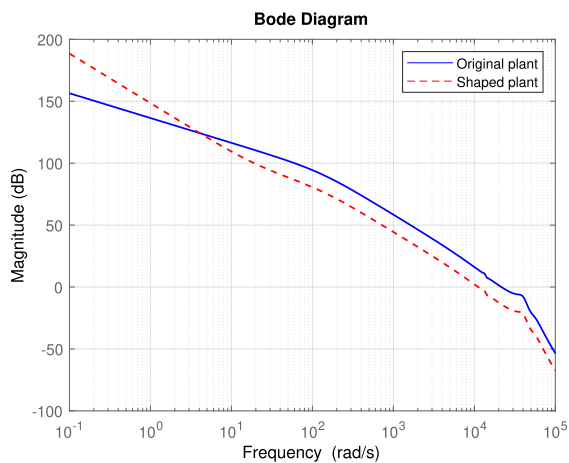

FIGURE 8. Frequency responses of the system and frequency-shaped HDD system.

Fig. 8 illustrates the bode plot of the original and frequency-shaped HDD systems. The plot reveals how the H_∞ loop-shaping design technique modifies the system's frequency response to achieve desired performance objectives. The solid blue line representing the original plant shows the magnitude of the H_∞ open-loop response across a range of frequencies, while the dashed red line indicates the shaped plant after the loop-shaping controller has been applied. The degree of overlap between the two lines is notable, suggesting that the frequency shaping has been carefully designed to maintain the system's inherent characteristics while enhancing certain aspects of its frequency response.

Fig. 9 presents the bode plots for a series of controllers of different orders. The plot is divided into two parts: the top graph shows the magnitude in decibels (dB), and the bottom graph shows the phase in degrees. Each line color represents a controller of a different order, ranging from the 6th to the maximum order considered.
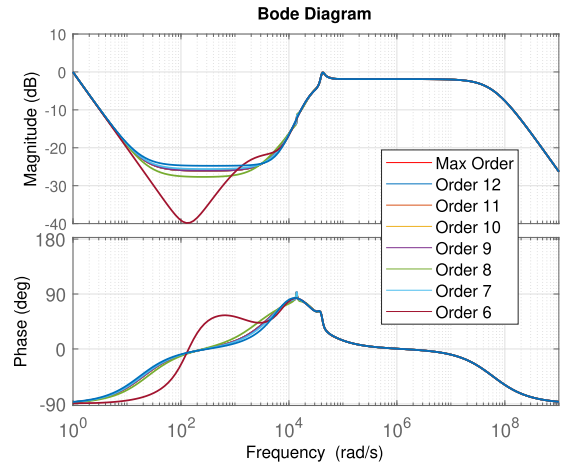

FIGURE 9. Orderwise Controller Bode plots.

In controller transfer function analysis equations (23)-(30) appear to be the transfer functions of the designed controllers for various orders.

$$TF_6(s) = \frac{\begin{array}{c}4.856 \times 10^7 s^5 + \\ 1.079 \times 10^{12} s^4 + 8.288 \times 10^{16} s^3 + \\ 8.022 \times 10^{20} s^2 + 3.25 \times 10^{24} s + \\ 5.569 \times 10^{25}\end{array}}{\begin{array}{c}s^6 + 6.036 \times 10^7 s^5 + \\ 2.819 \times 10^{12} s^4 + 1.543 \times 10^{17} s^3 + \\ 4.052 \times 10^{21} s^2 + 5.604 \times 10^{25} s\end{array}}, \qquad (23)$$

$$TF_7(s) = \frac{\begin{array}{c}4.856 \times 10^7 s^6 + 1.09 \times 10^{12} s^5 + \\ 8.391 \times 10^{16} s^4 + 8.332 \times 10^{20} s^3 + \\ 4.862 \times 10^{24} s^2 + 8.567 \times 10^{26} s + \\ 8.208 \times 10^{28}\end{array}}{\begin{array}{c}s^7 + 6.036 \times 10^7 s^6 + \\ 2.834 \times 10^{12} s^5 + 1.558 \times 10^{17} s^4 + \\ 4.136 \times 10^{21} s^3 + 5.89 \times 10^{25} s^2 + \\ 8.26 \times 10^{28} s\end{array}}, \qquad (24)$$

$$TF_8(s) = \frac{\begin{array}{c}4.856 \times 10^7 s^7 + 1.227 \times 10^{12} s^6 + \\ 9.645 \times 10^{16} s^5 + 1.326 \times 10^{21} s^4 + \\ 2.078 \times 10^{25} s^3 + 2.031 \times 10^{29} s^2 + \\ 6.994 \times 10^{32} s + 1.322 \times 10^{34}\end{array}}{\begin{array}{c}s^8 + 6.036 \times 10^7 s^7 + \\ 2.995 \times 10^{12} s^6 + 1.767 \times 10^{17} s^5 + \\ 5.1 \times 10^{21} s^4 + 1.028 \times 10^{26} s^3 + \\ 8.945 \times 10^{29} s^2 + 1.33 \times 10^{34} s\end{array}}, \qquad (25)$$

$$TF_9(s) = \frac{\begin{array}{c}4.856 \times 10^7 s^8 + 2.027 \times 10^{12} s^7 + \\ 1.239 \times 10^{17} s^6 + 3.033 \times 10^{21} s^5 + \\ 5.919 \times 10^{25} s^4 + 6.093 \times 10^{29} s^3 + \\ 6.717 \times 10^{33} s^2 + 1.494 \times 10^{37} s + \\ 3.589 \times 10^{38}\end{array}}{\begin{array}{c}s^9 + 6.038 \times 10^7 s^8 + \\ 4.004 \times 10^{12} s^7 + 2.332 \times 10^{17} s^6 + \\ 8.521 \times 10^{21} s^5 + 2.065 \times 10^{26} s^4 + \\ 3.499 \times 10^{30} s^3 + 3.29 \times 10^{34} s^2 + \\ 3.612 \times 10^{38} s\end{array}}, \qquad (26)$$

$$TF_{10}(s) = \frac{\begin{matrix} 4.856 \times 10^7 s^9 + 2.172 \times 10^{12} s^8 + \\ 2.704 \times 10^{17} s^7 + 7.137 \times 10^{21} s^6 + \\ 3.495 \times 10^{26} s^5 + 5.09 \times 10^{30} s^4 + \\ 7.044 \times 10^{34} s^3 + 7.031 \times 10^{38} s^2 + \\ 2.208 \times 10^{42} s + 4.387 \times 10^{43} \end{matrix}}{\begin{matrix} s^{10} + 6.038 \times 10^7 s^9 + \\ 4.186 \times 10^{12} s^8 + 4.207 \times 10^{17} s^7 + \\ 1.803 \times 10^{22} s^6 + 7.576 \times 10^{26} s^5 + \\ 1.93 \times 10^{31} s^4 + 3.682 \times 10^{35} s^3 + \\ 3.163 \times 10^{39} s^2 + 4.415 \times 10^{43} s \end{matrix}}, \quad (27)$$

$$TF_{11}(s) = \frac{\begin{matrix} 4.856 \times 10^7 s^{10} + 2.179 \times 10^{12} s^9 + \\ 2.707 \times 10^{17} s^8 + 7.173 \times 10^{21} s^7 + \\ 3.505 \times 10^{26} s^6 + 5.136 \times 10^{30} s^5 + \\ 7.111 \times 10^{34} s^4 + 7.124 \times 10^{38} s^3 + \\ 2.3 \times 10^{42} s^2 + 3.343 \times 10^{44} s + \\ 5.771 \times 10^{45} \end{matrix}}{\begin{matrix} s^{11} + 6.038 \times 10^7 s^{10} + \\ 4.194 \times 10^{12} s^9 + 4.212 \times 10^{17} s^8 + \\ 1.808 \times 10^{22} s^7 + 7.6 \times 10^{26} s^6 + \\ 1.94 \times 10^{31} s^5 + 3.707 \times 10^{35} s^4 + \\ 3.211 \times 10^{39} s^3 + 4.457 \times 10^{43} s^2 + \\ 5.807 \times 10^{45} s \end{matrix}}, \quad (28)$$

$$TF_{12}(s) = \frac{\begin{matrix} 4.856 \times 10^7 s^{11} + 2.181 \times 10^{12} s^{10} + \\ 2.709 \times 10^{17} s^9 + 7.189 \times 10^{21} s^8 + \\ 3.509 \times 10^{26} s^7 + 5.156 \times 10^{30} s^6 + \\ 7.143 \times 10^{34} s^5 + 7.169 \times 10^{38} s^4 + \\ 2.347 \times 10^{42} s^3 + 5.299 \times 10^{44} s^2 + \\ 2.275 \times 10^{47} s + 4.357 \times 10^{48} \end{matrix}}{\begin{matrix} s^{12} + 6.038 \times 10^7 s^{11} + \\ 4.198 \times 10^{12} s^{10} + 4.215 \times 10^{17} s^9 + \\ 1.811 \times 10^{22} s^8 + 7.611 \times 10^{26} s^7 + \\ 1.945 \times 10^{31} s^6 + 3.719 \times 10^{35} s^5 + \\ 3.234 \times 10^{39} s^4 + 4.478 \times 10^{43} s^3 + \\ 8.636 \times 10^{45} s^2 + 4.384 \times 10^{48} s \end{matrix}}, \quad (29)$$

$$TF_{13}(s) = \frac{\begin{matrix} 4.856 \times 10^7 s^{12} + 2.182 \times 10^{12} s^{11} + \\ 2.709 \times 10^{17} s^{10} + 7.194 \times 10^{21} s^9 + \\ 3.511 \times 10^{26} s^8 + 5.163 \times 10^{30} s^7 + \\ 7.153 \times 10^{34} s^6 + 7.183 \times 10^{38} s^5 + \\ 2.362 \times 10^{42} s^4 + 5.768 \times 10^{44} s^3 + \\ 2.381 \times 10^{47} s^2 + 8.907 \times 10^{48} s + \\ 8.713 \times 10^{49} \end{matrix}}{\begin{matrix} s^{13} + 6.038 \times 10^7 s^{12} + \\ 4.199 \times 10^{12} s^{11} + 4.215 \times 10^{17} s^{10} + \\ 1.812 \times 10^{22} s^9 + 7.614 \times 10^{26} s^8 + \\ 1.946 \times 10^{31} s^7 + 3.723 \times 10^{35} s^6 + \\ 3.241 \times 10^{39} s^5 + 4.485 \times 10^{43} s^4 + \\ 9.532 \times 10^{45} s^3 + 4.557 \times 10^{48} s^2 + \\ 8.769 \times 10^{49} s \end{matrix}}. \quad (30)$$

The parameters in equations (23)-(30) have specific physical meanings related to the dynamics of the HDD system parameters. For example, the parameters of the system represent inertia, damping ratios, and torque constants, which

are critical for accurately modeling the system's behavior. While these parameters may appear large, they are essential for achieving the desired control performance. Moreover, they are implementable in HDD systems, as they have been derived from practical considerations and validated through simulations.
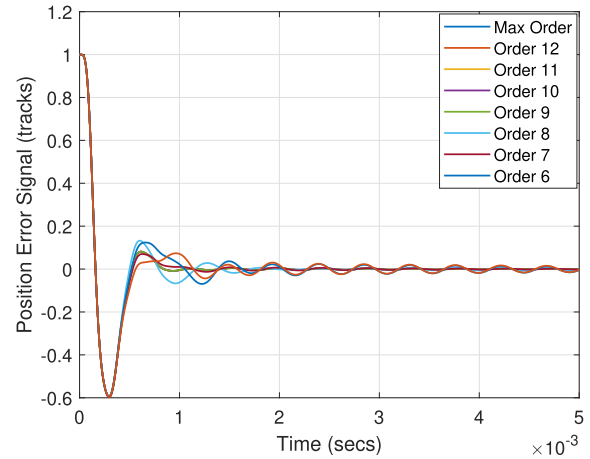

FIGURE 10. Closed-loop transient response.

Fig. 10 depicts the transient response of the HDD system's position error when following a reference command for various controller orders. The lines show how quickly and accurately the system responds to changes, which indicates the controller's performance in tracking tasks. Lower-order controllers tend to show more significant deviation from zero, suggesting less precise tracking than higher-order controllers, closely following the reference with minimal error.
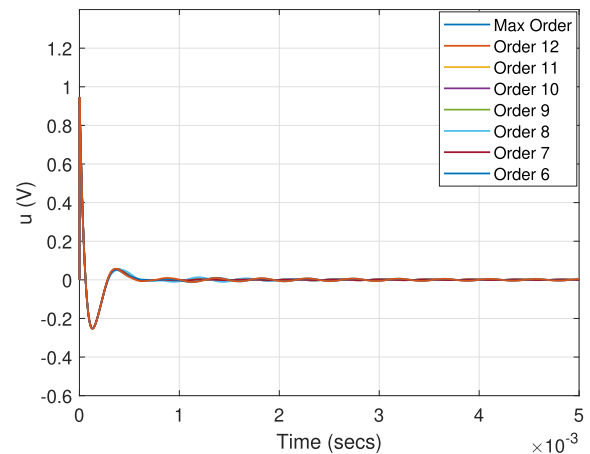

FIGURE 11. Control action, due to reference.

Fig. 11 demonstrates the control action, required by controllers of different orders to track a reference signal. It indicates how aggressively the controller acts to correct errors in the system's output. An ideal controller would provide a smooth control action without large spikes, which could lead to actuator saturation or increased wear and tear on the system.
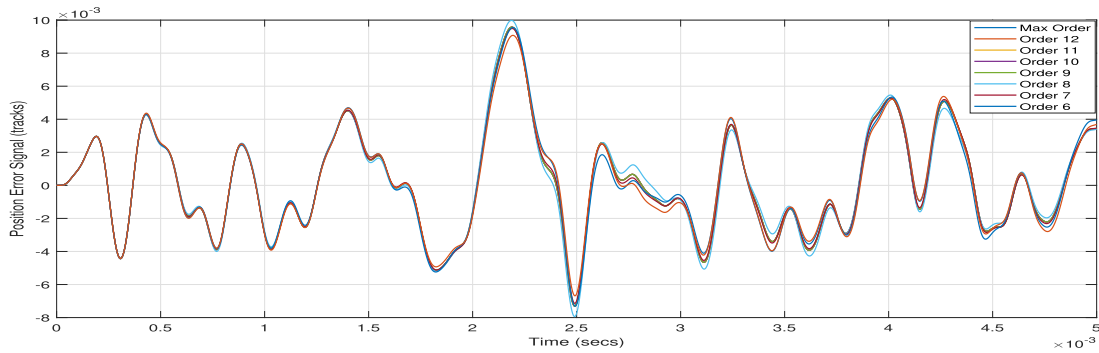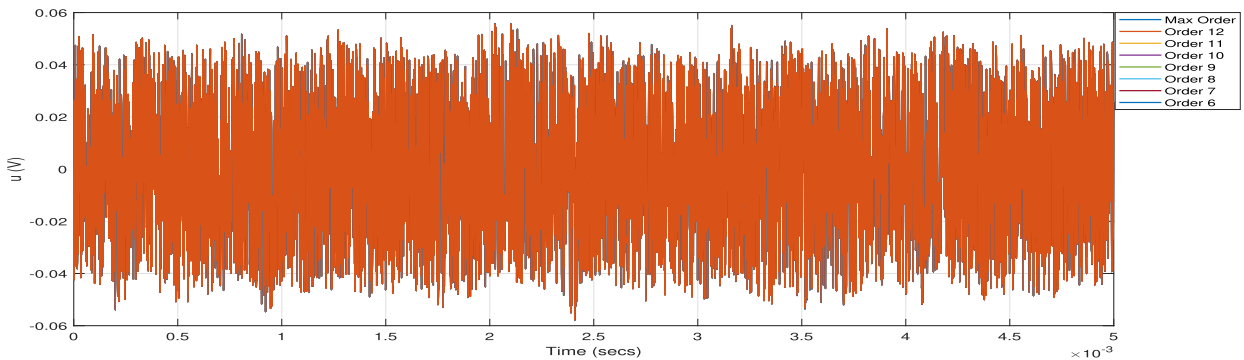
FIGURE 12. Transient response to noise.

FIGURE 13. Control action due to noise.

Fig. 12 shows the system's position error in response to noise, an important factor in real-world applications where sensor noise can affect performance. Controllers must filter out noise while still being responsive to actual system dynamics. The figure evaluates how well each controller order manages this trade-off.

Fig. 13 indicates the controller of each order reacts to sensor noise in terms of the control effort. Ideally, the controller should not react strongly to noise, as this can lead to unnecessary system actuation. This figure can help identify which controller orders are more susceptible to noise and may require additional filtering.

Fig. 14 The focus is on the system's robustness to external disturbances. The plot shows the position error due to disturbances for different controller orders. A well-designed controller would minimize the error and quickly return to a steady state, as indicated by the lines settling close to zero rapidly. It is essential for HDD systems where disturbances can significantly affect performance.

Fig. 15 reveals the corrective action taken by the controller to maintain the desired output despite external perturbations. The magnitude of the control signals gives insight into the disturbance rejection capabilities of each controller order.

Fig. 16 shows the performance metrics for controllers of different orders, specifically ITAE, ISE, and IAE. The x-axis represents the order of the controller, ranging from 6 to 13, while the y-axis shows the respective metric values.
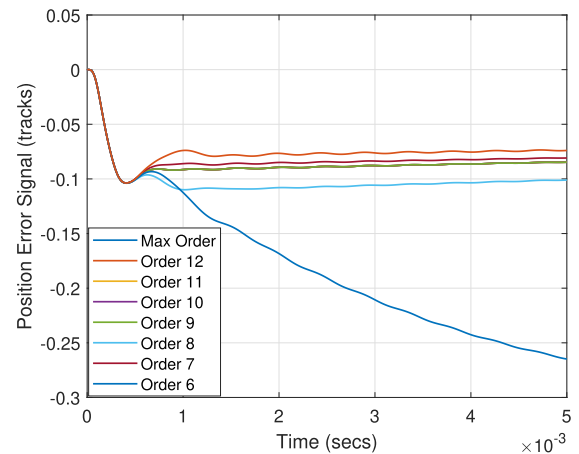

FIGURE 14. Transient response to disturbance.

The figure illustrates the trade-offs between controller complexity and performance. Higher-order controllers (11 and 12) exhibit slightly better transient performance and lower steady-state errors but come with increased computational complexity. The 10th-order controller provides a balanced performance with an optimal trade-off between computational efficiency and control accuracy, It will make it suitable for real-time applications and general industrial use. This analysis highlights the importance of selecting an appropriate controller order based on specific application requirements.
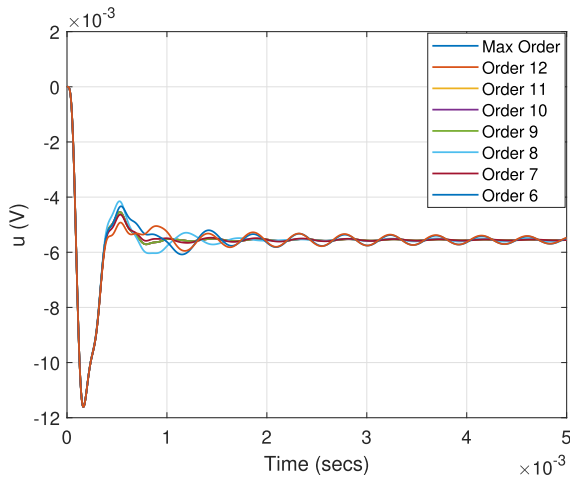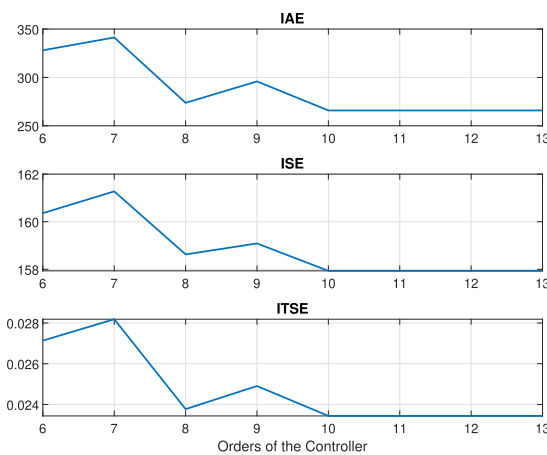
FIGURE 15. Control action due to disturbance.

FIGURE 16. Performance Metrics for Controllers of Different Orders.

A. SELECTION OF THE 10TH-ORDER CONTROLLER

The 10th-order controller demonstrated significant effectiveness in maintaining robust control while minimizing disturbances and noise. This was quantitatively evaluated using various performance metrics and simulation scenarios.

- **Robust Control:** The 10th-order controller maintained stability and effective control across a range of operating conditions, demonstrating robust performance in the presence of disturbances and noise. Figures 10 and 11 highlight the controller's ability to achieve quick settling times and minimal overshoot.
- **Minimizing Disturbances and Noise:** The controller effectively minimized the impact of external disturbances and sensor noise on the system's performance, as evidenced by the low position error and control action shown in Figs. 12 and 13.

A comprehensive analysis was conducted to evaluate the performance of controllers with various orders (6 through 13).

- **ITAE:** The 10th-order controller achieved the lowest ITAE value, indicating superior long-term error minimization (Fig. 16).

- **Transient Response:** Higher-order controllers (orders 11 and 12) showed slightly better transient performance, but the 10th-order controller provided a comparable balance with lower computational complexity (Figs. 10 and 14).
- **Control Effort:** The 10th-order controller required moderate control effort compared to higher-order controllers, which can lead to less actuator wear and energy consumption (Figs. 11 and 15).

The 10th-order controller offered an optimal trade-off between performance and complexity. While higher-order controllers provided marginally better performance, the increase in computational load was not justified given the minimal performance gains. This analysis supports the 10th-order controller's suitability for precision-critical industrial environments, effectively maintaining robust control while minimizing disturbances and noise.

B. CHALLENGES AND LIMITATIONS OF IMPLEMENTING SIMPLIFIED CONTROLLERS

Implementing simplified controllers in precision-critical industrial environments presents several challenges and limitations:

- **Precision and Accuracy:** Simplified controllers may not maintain the high precision required in critical applications, leading to slight but significant performance deviations.
- **Robustness to Variability:** Ensuring robust performance under variable conditions and disturbances in industrial environments can be challenging for simplified controllers.
- **Noise Sensitivity:** Simplified controllers may be less effective at filtering high-frequency noise compared to higher-order controllers, affecting system reliability.
- **Implementation and Tuning:** The complexity of implementing and tuning simplified controllers in real-world settings requires extensive testing and validation.
- **Compliance with Industry Standards:** Simplified controllers must meet industry standards and regulatory requirements, including safety, reliability, and performance standards.

C. MULTI-SCENARIO SIMULATIONS USING MATLAB

The robustness and adaptability of the controller were evaluated through multi-scenario simulations of the HDD system, focusing on uncertain system parameters and analyzing the controller's response.

- **Parameter Variations:** The simulations included variations in system parameters such as inertia, damping ratios, and torque constants to test the controller's robustness and adaptability.
- **Simulation Scenarios:** Different operating conditions were simulated by changing the model parameters. This approach allowed the assessment of the controller's

performance under consistent disturbances or noise conditions.

The controller maintained robust performance across different parameter variations, demonstrating its adaptability. The results showed that the simplified controller effectively handled changes in the HDD system dynamics.

- **Performance Metrics:** The effectiveness of the controller in these simulations was evaluated using the following performance metrics:

  ITAE: To assess long-term error minimization.
  Transient Response: To evaluate the system's quick response and stability.
  Control Effort: To measure the energy consumption and actuator load.

The multi-scenario simulations using MATLAB and Simulink validated the robustness and adaptability of the 10th-order H_∞ loop-shaping controller. These simulations underscore the controller's potential for reliable and efficient performance in diverse operational scenarios.

D. INVESTIGATION OF CONTROLLERS OF DIFFERENT ORDERS

The performance of controllers with varying orders (6 to 13) was investigated to identify the optimal controller order for different application scenarios.

Performance Metrics:

- **ITAE:** Assessed long-term error minimization.
- **ISE:** Evaluated error reduction efficiency.
- **IAE:** Measured overall error magnitude.

Findings:

- **Higher-Order Controllers:** Controllers of orders 11 and 12 showed slightly better transient performance and lower steady-state errors but increased computational complexity.
- **10th-Order Controller:** Provided a balance of performance and computational efficiency, It will make it suitable for real-time applications and general industrial use. Future work will focus on practical implementation and further optimization based on feedback.

V. CONCLUSION

This investigation corroborates the efficiency of a 10th-order H_∞ loop-shaping continuous-time controller for nonlinear HDD systems, optimized via Hankel-norm approximation. This controller demonstrated an optimal balance between performance and computational efficiency, excelling in robustness against disturbances and noise attenuation. The results, especially the ITAE metrics, validate the potential of reduced-order controllers for precision-demanding applications. This study lays the groundwork for deploying such controllers in high-accuracy industrial environments and prompts additional investigation of their applicability in diverse intricate control systems.

REFERENCES

[1] T. Atsumi and S. Yabui, "Loop-shaping technique for quadruple-stage actuator system in hard disk drive," *IEEE Trans. Ind. Appl.*, vol. 59, no. 4, pp. 5009–5018, Jul./Aug. 2023, doi: 10.1109/TIA.2023.3257135.

[2] K. Igarashi, R. Igarashi, T. Atsumi, and S. Nakadai, "Feedforward control for track seeking control in hard disk drive with sampled-data polynomial based on causal first-order hold," *IEEJ J. Ind. Appl.*, early access, May 3, 2024, doi: 10.1541/ieejjia.23008418.

[3] R. J. Caverly, M. Chakraborty, B. Huang, and R. Sosseh, "Robust mixed H_2-H_∞ control synthesis for dual-stage hard disk drives using convex optimization," *IFAC-PapersOnLine*, vol. 56, no. 2, pp. 10620–10625, 2023, doi: 10.1016/j.ifacol.2023.10.685.

[4] N. P. S. Prakash, J. Seo, J. Choi, and R. Horowitz, "Clustering techniques for stable linear dynamical systems with applications to hard disk drives," *IFAC-PapersOnLine*, vol. 56, no. 3, pp. 529–534, 2023, doi: 10.1016/j.ifacol.2023.12.078.

[5] S. Ibaraki and M. Tomizuka, "Tuning of a hard disk drive servo controller using fixed-structure H_∞ controller optimization," *J. Dyn. Syst., Meas., Control*, vol. 123, no. 3, pp. 544–549, Sep. 2001, doi: 10.1115/1.1386391.

[6] H. Murakami and S. Yabui, "Loop shaping method based on data considering mechanism constraints for each actuator in DISO magnetic head position control system in HDDs," in *Proc. IEEE 18th Int. Conf. Adv. Motion Control (AMC)*, Kyoto, Japan, Feb. 2024, pp. 1–6, doi: 10.1109/amc58169.2024.10505678.

[7] D.-B.-L. Douti, C. Ouro-Wassara, and E. Mabafei, "FriiTriga, a triggered controller with an optical beam shutter using a hard disk drive voice-coil actuator," *HardwareX*, vol. 19, Sep. 2024, Art. no. e00542, doi: 10.1016/j.ohx.2024.e00542.

[8] M. Mae, W. Ohnishi, and H. Fujimoto, "Frequency response data-based resonant filter design considering phase stabilization and stroke limitation applied to dual-stage actuator hard disk drives," *IFAC-PapersOnLine*, vol. 56, no. 2, pp. 10614–10619, 2023, doi: 10.1016/j.ifacol.2023.10.684.

[9] J. Velagic, A. Osmanovic, D. Koluh, and A. Karzic, "Adaptive control of hard disk drive servo system," in *Proc. Int. Symp. ELMAR*, Zadar, Croatia, Sep. 2020, pp. 91–96, doi: 10.1109/ELMAR49956.2020.9219044.

[10] N. O. P. Arancibia, T.-C. Tsao, and S. Gibson, "Adaptive tuning and control of a hard disk drive," in *Proc. Amer. Control Conf.*, New York, NY, USA, Jul. 2007, pp. 1526–1531, doi: 10.1109/acc.2007.4282928.

[11] S. Yabui, T. Atsumi, and T. Inoue, "Servo controller design for triple-stage actuator in HDD to compensate for high-frequency fan vibration," *IEEE Trans. Magn.*, vol. 58, no. 1, pp. 1–11, Jan. 2022, doi: 10.1109/TMAG.2021.3129540.

[12] M. Taktak-Meziou, A. Chemori, J. Ghommam, and N. Derbel, "Track following control using nonlinear model predictive control in hard disk drives," in *Proc. IEEE/RSJ Int. Conf. Intell. Robots Syst.*, Tokyo, Japan, Nov. 2013, pp. 4401–4406, doi: 10.1109/IROS.2013.6696988.

[13] K. R. Surur and M. Majid Gulzar, "Evolutionary based optimization techniques for compensating disturbances in R/W head positioning system of hard disk drives," in *Proc. Int. Conf. Control, Autom. Diagnosis (ICCAD)*, Paris, France, May 2024, pp. 1–6, doi: 10.1109/iccad60883.2024.10554052.

[14] A. K. Yadav, P. Saxena, P. Gaur, and P. K. Pathak, "Self-tuning fuzzy PID controller for servo control of hard disk drive with time delay," *Int. J. Inf. Technol.*, vol. 13, no. 1, pp. 109–114, Feb. 2021, doi: 10.1007/s41870-020-00567-w.

[15] T. Gao, C. Du, C. P. Tan, Z. He, J. Yang, and L. Xie, "High bandwidth control design and implementation for a dual-stage actuation system with a microthermal actuator," *IEEE Trans. Magn.*, vol. 49, no. 3, pp. 1082–1087, Mar. 2013, doi: 10.1109/TMAG.2012.2226187.

[16] S. Yabui, T. Atsumi, and T. Inoue, "Coupling controller design for MISO system of head positioning control systems in HDDs," *IEEE Trans. Magn.*, vol. 56, no. 5, pp. 1–9, May 2020, doi: 10.1109/TMAG.2020.2978156.

[17] A. A. H. Salah, K. Bouzrara, T. Garna, and H. Messaoud, "Controller order reduction techniques for loop shaping procedure," in *Proc. Int. Conf. Electr. Eng. Softw. Appl.*, Hammamet, Tunisia, Mar. 2013, pp. 1–5, doi: 10.1109/ICEESA.2013.6578417.

[18] D. Kumar, S. K. Nagar, and J. P. Tiwari, "Controller reduction using optimal Hankel norm approximation with guaranteed closed-loop performance," in *Proc. 7th IEEE Conf. Ind. Electron. Appl. (ICIEA)*, Singapore, Jul. 2012, pp. 757–762, doi: 10.1109/ICIEA.2012.6360826.

[19] I. Shaikh, E. W. Zerdazi, A. A. Wendimu, R. Matusu, S. Zarghoon, and S. Emebu, "Reduced-order loop-shaping controller design for nonlinear continuous-time HDD systems using Hankel-norm approximation," in *Proc. Conf. Control Syst. Optim. Control (CSOC)*, to be published.

[20] M. H. Marzaki, M. Tajjudin, M. H. F. Rahiman, and R. Adnan, "Performance of FOPI with error filter based on controllers performance criterion (ISE, IAE and ITAE)," in *Proc. 10th Asian Control Conf. (ASCC)*, Kota Kinabalu, Malaysia, May 2015, pp. 1–6, doi: 10.1109/ASCC.2015.7244851.

[21] D. W. Gu, P. Petkov, and M. M. Konstantinov, *Robust Control Design With MATLAB*. Berlin, Germany: Springer, 2005.

IBRAHIM SHAIKH was born in Kandi, India, in June 1993. He received the Bachelor of Technology and Master of Technology degrees in electrical engineering from Aliah University, Kolkata, India, with a focus on power systems and bidirectional dc-dc converters for hybrid electric vehicles. He is currently pursuing the Ph.D. degree with the Faculty of Applied Informatics, Tomas Bata University in Zlín, Czechia, specializing in robust controller design for LTI multivariable systems. He was an University Teaching Assistant and later a Lecturer in India. He has authored several impactful publications in control systems and automation technologies.

RADEK MATUŠŮ (Member, IEEE) was born in Zlín, Czech Republic, in 1978. He received the M.S. degree in automation and control technology in the consumer goods industry from the Faculty of Technology, Tomas Bata University (TBU) in Zlín, in 2002, and the Ph.D. degree in technical cybernetics from the Faculty of Applied Informatics (FAI), TBU in Zlín, in 2007. He was appointed as an Associate Professor of machine and process control with FAI, TBU in Zlín, in 2018. He has been holding various research or pedagogical positions with TBU in Zlín, since 2004, where he is currently a Researcher and the Project Manager. He has (co-)authored more than 50 scientific journal articles and more than 110 conference contributions. His research interests include the analysis and synthesis of robust control systems, fractional-order systems, and algebraic methods in control design. He is a member of the Topical Advisory Panel of Mathematics and Fractal and Fractional. He served as a Reviewer for more than 50 scientific journals, including *Automatica*, IEEE TRANSACTIONS ON AUTOMATIC CONTROL, and *IEEE Control Systems Magazine*. He serves as an Academic Editor for *Journal of Control Science and Engineering*. He was a Guest Editor of *Mathematical Problems in Engineering*.

EL WARDI ZERDAZI was born in Oran, Algeria, in June 1997. He received the B.Sc. degree in electrical and automation engineering from the University of Science and Technology Mohamed Boudiaf, Algeria, in 2018, and the M.Sc. degree in automation and industrial computing from the Faculty of Electrical Engineering, University of Science and Technology Mohamed Boudiaf, in 2020. Currently, he is pursuing the Ph.D. degree in automatic control and informatics with the Faculty of Applied Informatics, UTB. His master's thesis focused on modeling and controlling of cube robot-shaped inverted pendulum. He has worked as a Control System Engineer and an Algorithms University Assistant in Algeria, from 2020 to 2023. He is the author of several conference papers and journal articles in his research field. His research interests include robust control, under-actuated systems, nonlinear control, and adaptive.

ABEBE ALEMU WENDIMU was born in Jeldu, Ethiopia, in February 1993. He received the B.Sc. degree in electrical and computer engineering (industrial control) from Addis Ababa University, Ethiopia, in 2015, and the M.Sc. degree in automatic control and informatics in Industry 4.0 from the Faculty of Applied Informatics (FAI), Tomas Bata University (TBU) in Zlín, in 2023, where he is currently pursuing the Ph.D. degree in automatic control and informatics in Industry 4.0. He was a Flight Control Researcher and a Supervisor with the Information Network Security Administration (INSA), formerly known as the Information Network Security Agency, Ethiopia, from 2015 to 2021. His master's thesis focused on modeling and control of fractional order control for twin rotor MIMO systems. He is the author of several conference papers and journal articles in his research field. His research interests include fractional calculus, fractional-order control, and fractional-order identification.

• • •